Relationship between Measured 900 MHz Complex Impulse Responses and Topographical Map Data.

R.L. Kirlin, P.F. Driessen
Department of Electrical and Computer Engineering
University of Victoria
Victoria, B.C. Canada V8W 1P6
e-mail: peter@sirius.uvic.ca

Abstract: **1 GHz complex impulse response data in mountainous terrain is measured at closely spaced locations, and is processed as data from a synthetic aperture array. Experimental data from linear and crossed arrays with 50 or 100 elements is considered. The direction of arrival for each delayed component is identified, and contour plots of the receiver power at bearings and distances are produced. These coutour plots closely match the topography of the region, and clearly indicate that the strongest mountain reflections come from the steepest slopes.**

These results are used to establish a relationship between the mountain reflection coefficients and the topography, thus making it possible to invert the problem and estimate the impulse response (multipath delay profile) in mountainous terrain directly from topographical map data. Such estimates can help to select cell site locations and antenna configurations to minimize the delay spread.

I. INTRODUCTION

Our objective is to determine a method that allows topographic data bases to be converted to coverage maps usable for digital cellular radio systems. For such digital systems, two parameters (the multipath delay profile as well as the signal strength) will affect the received signal quality (bit error rate) and thus a useful coverage map will need to specify both parameters versus location. If the terrain is described as a collection of scatterers with known scattering coefficients (e.g. triangular reflectors from a topographic data base), and all paths from transmitter via each scatterer to receiver are defined, then in principle, both parameters may be determined, and may also be characterized statistically [1][2] However, it is necessary (and may be difficult) to accurately define the scattering coefficients (or cross-section) at the frequency of interest (e.g. 900 MHz) for each triangular region using only coutour, groundcover and mineral composition data.

Thus in this work, we seek to determine these scattering coefficients using measured complex impulse response data, and to locate the significant reflectors which contribute to the multipath delay profile. Measured impulse response data was collected at two sites in Vancouver, Canada (Figure 1) which include steep mountain slopes to the north, causing significant power in long delay multipaths at 1 GHz [3]. The data was recorded at complex baseband, using a 10 Mb/sec sliding correlator, thereby yielding complex impulse responses for the multipath channel with time resolution of 50 nsec.

A synthetic array was implemented using a precision positioner. This allows inversion of the data to correlate major reflections with topographic features. This is accomplished with a high-resolution spectrum or Direction-of- Arrival (DOA) estimator and knowledge of the delay time for each arrival, thereby creating the intersection of a DOA radial and an elliptical delay-time distance locus with transmitter and receiver as foci.

Results show clearly that significant reflectors can be located this way, and therefore their properties can be used in classification algorithms to classify topographic features for trial cell-sites at other locations. Although not tested, suggestions on how this might be accomplished are included.

Array processing began with tests of two schemes, conventional beamforming and minimum variance distortionless response (MVDR). MVDR (also referred to as Linear Constrained Minimum Variance (LCMV)) was subsequently selected as the preferred method due to its proper dimensioning to estimate the signal power from a given direction. The qualitative correlation of response data (specifically reflected power and reflector location) with topographic features results are very good. Overlays of reflected power vs $x - y$ location correspond highly with steep topography gradients.

II. ARRAY PROCESSING FUNDAMENTALS

A. Problem Formulation

0-7803-1927-3/94/$4.00

The signal received by a receiver in a mountainous area can be considered as a superposition of direct path signal and reflected radio waves. Let $s(t)$ be the base-band signal transmitted through a channel with impulse response $h(t)$, so that the received signal

$$r(t) = \int_{-\infty}^{\infty} s(t-\tau)h(\tau)d\tau \tag{1}$$

is determined by

$$h(t) = \sum_{k=0}^{D} \rho_k e^{j\phi_k}\delta(t-\tau_k) \tag{2}$$

where $\phi_k = -2\pi f_0 \tau_k$, f_0 is the rf carrier frequency, and $\tau_k = (r_{TS_k} + r_{S_kR})/c$ is the absolute delay of the path from T via the k-th scatterer S_k to R. A typical measured $|h(t)|^2$ is shown in Figure 2. For general terrain characterized by the normalized radar cross-section σ^0,

$$|\rho_k|^2 = \frac{\lambda^2}{(4\pi)^3}\int_A \frac{\sigma^0 dA}{r_{TS}^2 r_{SR}^2} \tag{3}$$

where the integral is evaluated as a sum by defining the elements of area dA for each scatterer S_k using a topographical data base, and an estimate of σ_k^0 for each scatterer. The sum is performed over all scatterers S_k for which $(r_{TS_k} + r_{S_kR})$ is constant within the distance resolution [3]. Assuming that $r(t)$ contains reflected signals from D scatterers, $r(t)$ can be modeled as the sum of D components

$$s_k(t) = \rho_k e^{j\phi_k} s(t) \qquad k = 1, 2, \ldots, D, \tag{4}$$

where ρ_k is the reflection coefficient and ϕ_k is the phase shift; both of them can be treated as independent random variables. Assume that data measured at M adjacent locations are used to form a synthetic aperture or an M sensor array. The array receives $D+1$ plane waves from D scatterers and one direct path. We further assume that the baseband signals, $s_k(t)$ have approximate constant amplitude during the time it takes for the wave to travel across the array. This assumption (narrow-bandness) enables modeling the time delays between receivers as phase shifts. Let $x_i(t)$ denote the complex representation of the signal at sensor i and $x(t)$ denote the array output vector with the ith element $x_i(t)$. Then the array output vector can be written by

$$x(t) = \sum_{k=0}^{D} a(\theta_k)s_k(t) + n(t), \tag{5}$$

where θ_k denotes the incident direction of the kth signal with $k = 0$ corresponding to the direct path, $a(\theta_k)$ denotes array manifold vectors

$$a(\theta_k) = e^{j2\pi\triangle k \sin(\theta) f_0/c} \tag{6}$$

with $\triangle$ is the distance between adjacent sensing elements, the direction θ is measured relative to the normal of the array (broadside), and $n(t)$ represents the additive measurement noise. A more compact expression of (5) is given by

$$x(t) = A(\theta)s(t) + n(t), \tag{7}$$

where

$$\theta = [\theta_0, \theta_1, \theta_2, \ldots, \theta_D]^T \tag{8}$$

$$A(\theta) = [a(\theta_0), a(\theta_1), a(\theta_2), \ldots, a(\theta_D)] \tag{9}$$

$$s(t) = [s_0(t), s_1(t), s_2(t), \ldots, s_D(t)]^T \tag{10}$$

Assuming that the noise is independent of the signal waveforms, the covariance matrix of the array output vectors is

$$R = E[x(t)x^H(t)] = A(\theta)SA(\theta) + N, \tag{11}$$

where S and N are the covariance matrices of the signals and noise, respectively. If only a finite observation is available, the sample covariance matrix can be used in place of the true covariance matrix.

B. DOA Estimation

More recently, the eigenvectors associated with the array covariance matrix have been employed to obtain high resolution DOA estimates. When using these methods, one must first form an estimate of the array covariance matrix from the sampled array outputs and then a generalized eigen-analysis of the matrix pair (R, N) is made, that is

$$Rv_i = \lambda_i N v_i \qquad \text{for} \quad 1 \le i \le M, \tag{12}$$

where v_i and λ_i are the eigenvector and eigenvalue of the matrix pair (R, N).

Subspace-based methods are those which explicitly or implicitly partition the vector space into signal and noise subspaces. The number of signals is determined by considering the distribution of the generalized eigenvalues. No matter which algorithm is used, the fact that the individual source steering vectors are orthogonal to each of the noise level eigenvectors is utilized to obtain the DOA estimates of the echo signals. For example, the MUSIC spectrum is given by

$$P(\theta) = \frac{1}{\sum_{i=D+2}^{M} ||a^H(\theta)v_i||^2}, \tag{13}$$

the peaks of which represent the MUSIC estimates of DOA's. The peaks correspond to trial θ that give $a(\theta)$ orthogonal to the M-D noise-space eigenvectors.

C. Spatial Smoothing

For subspace-based high resolution algorithms, accurate partition of the signal and noise subspace is crucial. If such a partition is not correctly done, these algorithms will totally fail to function. When there are some coherent signals present, or there is at least one signal which is a scaled version of another signal, the dimension of signal subspace will be reduced according to the number of coherent signal present. Thus subspace partition will inevitably be erroneous. In order to overcome this problem, spatial smoothing was proposed as a preprocessing scheme for subspace-based algorithms for a uniform linear array. Further array processing information appears in [4]-[8].

D. Waveform Estimation

In addition to the DOA information, we are also interested in range, scatterer's signature and channel impulse response due to each scatterer. If the signal waveform from each individual scatterer or scattering region can be extracted, the information required should be easily obtained. The traditional means of doing this is beamforming [9], where a beam is formed artificially by electronic steering. The output of a beamformer is the linear combination of array output

$$y(t) = w^H x(t). \tag{14}$$

Beamformer algorithms differ only in the method of choosing the weighting vector w. With the DOA estimation available, the linearly constrained minimum variance beamformer (LCMV) is suitable for waveform estimation. To design a LCMV beamformer to extract the ith signal, a constraint matrix C is formed such that the array response to the remaining D signals are nulls while allowing the ith signal to pass without attenuation or

$$C^H w = f, \tag{15}$$

where

$$\begin{aligned} C &= [a(\theta_0), a(\theta_1), \ldots, a(\theta_{i-1}), a(\theta_i), a(\theta_{i+1}), \ldots, a(\theta_D)] \\ f &= [0, 0, \ldots, 0, 1, 0, \ldots, 0]^T. \end{aligned} \tag{16}$$

The determination of the optimal weighting vector becomes the constrained minimization problem of

$$w = \text{argmin}_w w^H R w \qquad \text{subject to} \qquad C^H w = f, \tag{17}$$

and it is found to be

$$w = R^{-1} C [C^H R C]^{-1} f. \tag{18}$$

An alternative approach for waveform estimation is to employ least squares (LS) methods and waveforms corresponding to all signals can be obtained simultaneously. We have successfully applied the LS methods to interference cancellation in seismic signal processing. Specifically, there are two LS solutions; stochastic and deterministic LS solutions. The stochastic LS estimate of $s(t)$ is given by

$$s_{sls}(t) = S A^H(\theta) R^{-1} x(t), \tag{19}$$

where S is signal covariance matrix, and it can be estimated by

$$S = A^{\#}(\theta)(R - N)A^{\#*}(\theta), \tag{20}$$

with $A^{\#}(\theta)$ denoting the pseudo-inverse of $A(\theta)$.

The deterministic LS solution is

$$s_{dls}(t) = A^{\#} x(t), \tag{21}$$

E. Preliminary Tests

The MUSIC method outlined in Section II.B was tested on the array data. Since the recorded data is complex demodulated to base band, the phase information retained in the demodulated signal contains the carrier phase information; i.e., the phase change between each trace is actually the relative carrier phase shift at 910 MHz. This makes the application of simple narrow- band MUSIC possible.

It can be shown that the covariance of the demodulated PN sequence at the ith and jth sensors (traces) is:

$$E[s(t - \tau_i)s(t - \tau_j)\exp(j 2\pi f_0(\tau_i - \tau_j))] \tag{22}$$

where τ_i and τ_j are the delay at the ith and jth traces, and f_0 is carrier frequency. This verifies that the direction vector should incorporate the carrier frequency (910 MHz). That is, the phase difference between two sensors should be $2\pi f_0 d_{ij}$ with f_0 being the carrier frequency and d_{ij} the delay between ith and jth traces. The complex number in the i, jth element of cov $[x]$ will have phase angle (for a single wavefront) equal to $2\pi f d_{ij}$. Knowing the carrier frequency, we can deduce the delay and arrival angle from the sample.

Using MUSIC, we form one covariance matrix for each time window position (short around each trial path delay), and do not change that window location for different trial angles of arrival. That is, we may determine multiple DOA's near each delay time with only one window, utilizing a number of time slices $\underline{x}_j$ to get cov $[x]$.

III. REFLECTOR LOCATION ESTIMATION

A direction finding algorithm like MVDR or MUSIC is used for DOA. The delay time between transmitter and receiver can be used to determine an ellipse with foci at the transmitter and receiver locations. Together the DOA and time delay ellipse determine the reflector location. Time delay of course translates to distance. A change of coordinates eventually relates the reflector position to that of the transmitter. The angle vs distance results are converted into distance vs distance plots, in order to coordinate the actual points of reflection with a topographical map.

The results of BF processing for the Capilano/Park Royal data have been plotted to the same scale as a topographic map of the region. These plots (Figures 3, 4) are then made into overlays to observe the regions of reflectance from the topographical map, Figure 1. Interesting responses follow significant topo contour gradients even back into a canyon due north. NS array results are similar, but show the expected front-back ambiguity.

When one positions the overlays on top of the provided topographical map, making sure that the North-South directions are aligned properly such that the point (0, 0) on the overlay lies on the center of the "cross" on the map, one can see the major sources of the reflection. One of the more impressive regions to notice is the area near Grouse Mountain. Near the bottom of Grouse Mountain, beside the lake, there are very steep and jagged cliff formations, most likely causing the concentration of the power in that region. Looking at the "W to E" overlay, one can observe how well the contours of the surrounding topography are closely mapped to the Source Reflectance contours.

IV. SUMMARY

The results reported above are very encouraging. The method and results of processing of cross-array data (two orthogonal linear arrays), phase drift correction, center element location are omitted for lack of space.

Howver, much work remains to be done. It is the long term goal of this research to produce an algorithm which predicts channel response in a coverage area. Most literature on the subject deals with deterministic approaches using direct paths and paths of similar delay from known or hypothesized objects, surfaces or structures, for example [1]. These approaches involve extensive calculations, incorporating numerical solutions to equation like those in Section 2.

We are suggesting that all potential reflecting incremental surfaces may be preclassified by its features, thereby excluding all but a small proportion from the final estimation of the channel response. A suggested methodology for quickly determining regions of reflecting surfaces which are likely to cause significant reflections is omitted for lack of space. How large a training set should be found to instruct the classifier and what parameters should be used, aside from the obvious ones, needs further study. We also expect that a number of refinements must be added to the method we have outlined. Nevertheless we are confident that further research merging the array inversion methods with classification can lead to quick solutions to cell site design and coverage prediction.

V. REFERENCES

[1.] Lebherg, M., W. Wiesbeck and W. Krank, "A versatile wave propagation model for the VHF/UHF range considering three-dimensional terrain", IEEE Trans. Antennas and Propagation, vol. 40, pp. 1121-1131, 1992.

[2.] Braun, Walter R. and Ulrich Dersch, "A physical mobile radio channel model", IEEE T-Vehic. Tech., 40, No. 2, pp. 472-482, May 1991.

[3.] Driessen, P.F., "Multipath delay characteristics in mountainous terrain at 900 MHz", *Proc. IEEE Vehic. Tech. Conf.*, Denver, May 1992, pp. 520-523.

[4.] Drosopoulos, A. and S. Haykin, "Experimental characterization of diffuse multipath at 10.2 GHz using method of multiple windows", *IEE Electronics Letters*, Vol. 27, No. 10, pp. 798-799, May 1991.

[5.] Marple, S.L., Jr., *Digital spectral analysis with applications*, Prentice-Hall, INC., 1987.

[6.] Evans, J.E., J.R. Johnson and D.F. Sun, "Application of advanced signal processing techniques to angle of arrival estimation in ACT navigation and surveillance systems", M.I.T. Lincoln Lab., Lexington, MA, Tech. Rep. 582, June 1982.

[7.] Friedlander, "Direction finding using an interpolated array", IEEE Proceedings, ICASSP, 1990.

[8.] Kirlin, R.L. and W. Du, "Design of transformation matrices for array processing", Proc. IEEE Int. Conf. Acoustics, Speech & Signal Processing, ICASSP-91, pp. 1389-1392, May 1991.

[9.] Neidell, N.S. and M.T. Taner, "Semblance and other coherency measures for multi-channel data", vol. 26, No. 3, pp. 482-497, 1971.

Figure 1. Topographical map of Vancouver, Canada.

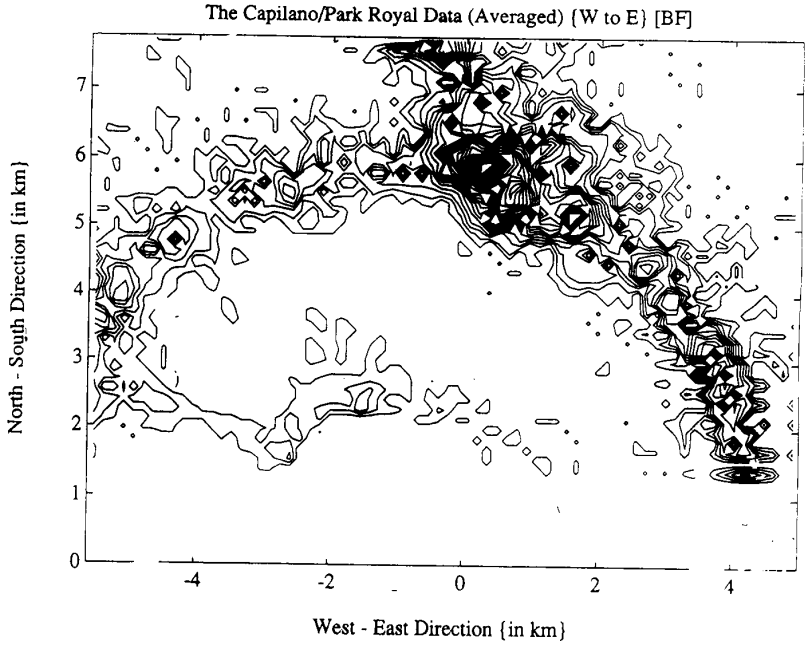

Figure 2. NS array BF results, to scale for overlay on Figure 1.